



HAL
open science

Interaction of Cisplatin with 5'-dGMP: A Combined IRMPD and Theoretical Study

Barbara Chiavarino, Maria Elisa Crestoni, Simonetta Fornarini, D. Scuderi,
Jean-Yves Salpin

► **To cite this version:**

Barbara Chiavarino, Maria Elisa Crestoni, Simonetta Fornarini, D. Scuderi, Jean-Yves Salpin. Interaction of Cisplatin with 5'-dGMP: A Combined IRMPD and Theoretical Study. *Inorganic Chemistry*, 2015, 54 (7), pp.3513-3522. 10.1021/acs.inorgchem.5b00070 . hal-01221291

HAL Id: hal-01221291

<https://hal.science/hal-01221291>

Submitted on 5 Oct 2018

HAL is a multi-disciplinary open access archive for the deposit and dissemination of scientific research documents, whether they are published or not. The documents may come from teaching and research institutions in France or abroad, or from public or private research centers.

L'archive ouverte pluridisciplinaire **HAL**, est destinée au dépôt et à la diffusion de documents scientifiques de niveau recherche, publiés ou non, émanant des établissements d'enseignement et de recherche français ou étrangers, des laboratoires publics ou privés.

Interaction of cisplatin with 5'-dGMP: a combined IRMPD and theoretical study

Barbara Chiavarino^{1}, Maria Elisa Crestoni¹, Simonetta Fornarini¹, Debora Scuderi^{2,3} and Jean-Yves Salpin^{4,5*}*

1) Dipartimento di Chimica e Tecnologia del Farmaco, Università di Roma “La Sapienza”, P.le A. Moro 5, I-00185 Roma, ITALY

2) Université Paris Sud Orsay – Laboratoire de Chimie-Physique – Avenue Georges Clémenceau – 91405 Orsay Cedex – FRANCE

3) CNRS- UMR 8000.

4) Université d'Evry Val d'Essonne – Laboratoire Analyse et Modélisation pour la biologie et l'Environnement – Boulevard François Mitterrand – 91025 Evry – FRANCE

5) CNRS- UMR 8587.

Corresponding authors:

Dr Barbara Chiavarino
e-mail: barbara.chiavarino@uniroma1.it

Dr Jean-Yves Salpin
e-mail: jean-yves.salpin@univ-evry.fr

Abstract

IR Multiple Photon Dissociation (IRMPD) spectroscopy of cis -[Pt(NH₃)₂(5'-dGMP-H)]⁺ and cis -[PtCl(NH₃)₂(5'-dGMP)]⁺ ions (where (5'-dGMP) is 2'-deoxyguanosine-5'-monophosphate), generated in the gas phase by electrospray ionization, has been performed in two spectral regions, namely 700-1900 cm⁻¹ and 2800-3800 cm⁻¹. For structural assignment, experimental IRMPD spectra were compared to IR spectra computed at the B3LYP/LACV3P/6-311G** level of theory. In agreement with computational results, the vibrational spectroscopic characterization of the cis -[Pt(NH₃)₂(5'-dGMP-H)]⁺ ion points to macrochelate species resulting from the simultaneous interaction of the metal with both the N7 atom of the guanine residue and an O atom of the phosphate group, structures that bear feature in common with those characterized in solution by NMR spectroscopy. Concerning the cis -[PtCl(NH₃)₂(5'-dGMP)]⁺ ion, our study points to a monodentate complex involving exclusively the N7 position of guanine, as observed in solution. Also this species exhibits a compact form due to the formation of two hydrogen bonds involving the same ammonia ligand. For both complexes, IRMPD experiments show that a strong intramolecular hydrogen bond is established between one ammonia hydrogen and the carbonyl group of guanine. The strength of this particular interaction can be qualitatively estimated by looking at the redshift of the CO vibration with respect to an unperturbed C=O stretching mode in the fingerprint region. This point is also highlighted in the X-H (X= N,O) stretch region, by the shift of the N-H stretch frequency as a function of the number of hydrogen bonds involving the ammonia ligand.

Introduction.

Cisplatin (*cis*-diamminedichloroplatinum(II)) has been one of the most widely prescribed drug for many cancer diseases, especially against testicular, ovarian, head, and neck cancer.¹ Although its mechanism of action has not yet been fully elucidated, it is generally accepted that the therapeutic activity of cisplatin is achieved by binding with DNA to form crosslinks as major lesions, thus inhibiting replication and transcription processes and finally the cell's repair mechanism.²⁻⁵

With this paper, we continue the experimental structural characterization of ionic complexes from cisplatin and DNA components in the gas phase by combining IRMPD (Infrared Multiple Photon Dissociation) spectroscopy of complexes generated in a mass spectrometer by electrospray ionization (ESI), to theoretical DFT calculations. As illustrated by our previous studies, we chose a strategy based upon the gradual increase of the size of the nucleic acid building blocks. We have first characterized the biologically active form of cisplatin, namely *cis*-[PtCl(NH₃)₂(H₂O)]⁺, formed within the cell by a ligand exchange process promoted by the low intra-cell chloride concentration.⁶ We have then provided a detailed characterization of the *cis*-[PtCl(NH₃)₂(G)]⁺ and *cis*-[PtCl(NH₃)₂(A)]⁺ complexes (where G is guanine and A is adenine), the simplest models of the monofunctional adducts between cisplatin and the nucleobases of DNA.⁷

Proceeding with increasing complexity of the ligand, we presently report a study of the interaction of cisplatin with 2'-deoxyguanosine-5'-monophosphate (5'-dGMP). Moving from the simple nucleobase to the mononucleotide, the possible binding sites of cisplatin increase. In addition to the N7 position of guanine, platinum may interact with the oxygen(s) of the phosphate group and with the hydroxyl group of the deoxyribose moiety. Figure 1 shows the structure of 5'-dGMP. Due to the greater flexibility of the nucleotide as compared to the

nucleobase, many conformers are possible depending in particular on the rotation of the nucleobase about the *N*-glycosidic bond and on the ribose ring-puckering. As a matter of fact, the nucleotide may be either in *syn* (*anti*) conformation when the amino group of the G residue is oriented toward (away from) the phosphate group. Regarding the sugar ring-puckering, the “south” (S) structures are those with the C2'-endo conformation, while the “north” (N) ones present a C3'-endo conformation.

< Figure 1 >

Two ions were presently considered for their structural characterization by IRMPD spectroscopy, namely the $cis\text{-[Pt(NH}_3)_2(5'\text{-dGMP-H)]}^+$ and $cis\text{-[PtCl(NH}_3)_2(5'\text{-dGMP)]}^+$ complexes. The former has been previously characterized by a combined NMR and theoretical study.^{8,9} Results of these previous studies have postulated a macrochelate structure for the $cis\text{-[Pt(NH}_3)_2(5'\text{-dGMP)-H]}^+$ complex, where the nucleotide is bound to the $cis\text{-[Pt(NH}_2\text{R)}_2]$ moiety (R= H, CH₃) via N7 and an O of the phosphate group, with a *anti* orientation of the nucleobase and a strong preference for an North sugar conformation. The characterization of $cis\text{-[PtCl(NH}_3)_2(5'\text{-dGMP)]}^+$, that models the first species resulting from attack of cisplatin to DNA, is more complicated. $cis\text{-[PtCl(NH}_3)_2(5'\text{-dGMP)]}^+$ is a transient complex which further reacts for example by loss of HCl. In a previous NMR study of this particular complex, the lack of protonation onto the N7 position of GMP indicated that platinum was bound to the N7 atom of the guanine residue.^{10,11} Presently, the use of ESI coupled to mass spectrometry in order to isolate the complex of interest generated in solution is very helpful for studying short-lived ions in the gas phase.¹²⁻¹⁵ Furthermore, the coupling of a mass spectrometer to intense infrared sources allows one to obtain the structural characterization of the ion of interest. Two distinct energy ranges were considered. First,

IRMPD spectra were recorded in the fingerprint region (700-1900 cm^{-1}) using an IR free electron laser. Subsequently, the vibrational modes associated with the CH, NH and OH stretches were also investigated by recording IRMPD spectra in the 2800-3800 cm^{-1} frequency range, using an optical parametric oscillator (OPO/OPA) laser. The latter spectral range is of particular interest for probing the vibrational shifts associated with stretches involved in hydrogen bonds.

Experimental

2.1 Materials

Cisplatin and 5'-dGMP used in this work were research grade products from commercial sources (Sigma-Aldrich s.r.l. Milan, Italy) and were used without further purification. In order to generate the complexes of interest, stock solutions of either cisplatin or 5'-dGMP, both in the mM range in purified water, were prepared, mixed in 1:1 molar ratio and diluted with water to reach the final concentration of $5 \cdot 10^{-5} \text{M}$ in each analyte..

2.2 IRMPD experiments

The complexes of interest have been obtained as gaseous species by ESI of water solutions prepared as described. Typical ESI conditions were a flow rate of 2-4 $\mu\text{L}/\text{min}$, capillary spray voltage at -4.5 kV , nebulizer at 12 PSI, drying gas flow at 5 L/min , and drying gas temperature at 300°C .

IRMPD spectroscopy in the 700-1900 cm^{-1} frequency range (the so-called fingerprint region) has been performed at the beamline of the free electron laser (FEL) of the Centre Laser Infrarouge d'Orsay (CLIO). For the present study, the electron energy of the FEL was set at 36 and 45 MeV in two distinct runs, in order to optimize the laser power in the frequency

region of interest. FEL-based experiments were performed by coupling of the FEL beamline with a hybrid FT-ICR tandem mass spectrometer (APEX-Qe Bruker Daltonics)^{16,17}, equipped with a 7.0 T actively shielded magnet and a quadrupole-hexapole interface for mass-filtering and ion accumulation, under the control of the commercial software APEX 1.0. Mass selection of the *cis*-[PtCl(NH₃)₂(5'-dGMP)]⁺ and *cis*-[Pt(NH₃)₂(5'-dGMP)-H]⁺ ions was performed in the quadrupole, and ions were accumulated in the hexapole containing argon (buffer gas) for 0.5 s for collisional cooling prior to their transfer into the ICR cell. The isolated charged complexes were then irradiated for 100 ms to 420 ms with the IR FEL light, after which the resulting ions were mass-analyzed.

To record the spectra of the different complexes in the 2800-3800 cm⁻¹ spectral region, an Optical Parametric Oscillator/Amplifier (OPO/OPA) (LaserVision) laser system coupled to a Paul ion trap mass spectrometer (Esquire 6000+, Bruker Daltonics), has been employed as described previously.¹⁸ The typical output energy from the OPO/OPA laser was 20 mJ/pulse in the investigated spectral range with 3-4 cm⁻¹ bandwidth. In the trap, ions were mass-selected and accumulated for 5-10 ms prior to IR irradiation. The irradiation time used in the experiment varies from 0.5 to 4 s.

IRMPD spectra are obtained by plotting the photofragmentation yield R ($R = -\ln[I_{\text{parent}}/(I_{\text{parent}} + \sum I_{\text{fragment}})]$), where I_{parent} and I_{fragment} are the integrated intensities of the mass peaks of the precursor and of the fragment ions, respectively) as a function of the frequency of the IR radiation.¹⁶ A recent study has established that this data treatment gives better comparison with calculated infrared absorption spectra and a better spectral resolution than other analysis methods, such as calculating a photodissociation yield or recording a depletion spectrum of the parent ion abundance.¹⁹

2.3 Computational Details

Molecular orbital calculations were carried out using the B3LYP density functional,^{20,21} as implemented in the Gaussian-09 set of programs.²² The different species considered have been optimized using the 6-311G** basis set, without any symmetry constraint. In order to describe the metallic center, we used the Los Alamos effective core potential (ECP) in combination with the LACV3P** basis set.²³⁻²⁵ Harmonic vibrational frequencies were estimated at this level in order to characterize the stationary points as local minima or saddle points, and to estimate the zero-point vibrational energy (ZPE) corrections. In the perspective of studying bigger systems, B3LYP/6-31G** calculations have been also performed, Pt being described either with the SKBJ ECP+basis sets²⁶ or the LANL2DZ approach.²³⁻²⁵ It turned out that both the relative energies and vibrational spectra are similar, regardless of the pseudo-potential and basis sets used to perform the calculations.

The infrared absorption spectra of the various structures were calculated within the harmonic approximation. All calculated frequencies were scaled by a factor of 0.974 and 0.957 in the fingerprint and X-H stretch regions, respectively, for a better agreement with the experimental spectrum. These scaling factor were previously adopted for the related simpler complexes *cis*-[PtCl(NH₃)₂G]⁺ and *cis*-[PtCl(NH₃)₂A]⁺, with good results.⁷ However, a separate discussion is required for the IR modes involving the phosphate group. As reported in previous papers, the scaling factors generally adopted for the other vibrations are systematically too low for the vibrational modes of the P–OC, P–OH and P=O bonds belonging to the phosphate group, when compared to the experimental frequencies. This has been recently noticed during the study of different biomolecular ions, such as phosphorylated amino acids,^{27 28} peptides,²⁹ and nucleotides.³⁰⁻³² In a recent publication,³² a scaling factor of 0.974 was chosen for the vibrations above 1300 cm⁻¹, and no scaling for vibrations below 1300 cm⁻¹, the phosphate (P–

OH, P=O and P–OC) stretches region. In all the cases reported, it seems that the scaling factor should be even greater than one. Given these considerations, we decided in the present study to use a scaling factor of 0.974 for all the IR frequencies in the fingerprint region, and no scaling factor (that is 1) only for the frequencies involving the P=O, P–OH and P–OC modes of the phosphate group. For the sake of comparison with experimental data, calculated IR spectra were convoluted with a lorentzian profile of 20 cm^{-1} (fwhm) in the fingerprint region and of 5 cm^{-1} in the in the X-H stretch region.

Throughout this paper, total energies are expressed in Hartrees and relative energies in kJ mol^{-1} . For the sake of simplicity, the basis set used will be referred to as 6-311G** henceforth. Detailed geometries (Cartesian coordinates) of all the structures mentioned in this paper are available from the authors upon request.

3. Results and Discussion

Formation of both *cis*-[PtCl(NH₃)₂(5'-dGMP)]⁺ and *cis*-[Pt(NH₃)₂(5'-dGMP–H)]⁺ adducts is obtained upon mixing the two solutions containing cisplatin and 2'-deoxyguanosine-5'-monophosphate. When a solution of cisplatin and 5'-dGMP in 1:1 ratio is analysed, soon after mixing, under usual ESI conditions, an intense signal is observed at *m/z* 610-614 consistent with the formation of *cis*-[PtCl(NH₃)₂(5'-dGMP)]⁺. A second albeit less abundant ion at *m/z* 574-578 corresponding to the *cis*-[Pt(NH₃)₂(5'-dGMP–H)]⁺ complex is also present in the mass spectrum. After 24 h, the *cis*-[Pt(NH₃)₂(5'-dGMP–H)]⁺ complex becomes predominant. The complexes of interest are formed together with other species containing 5'-dGMP derivatives bound with cisplatin ions, as reported previously.⁷ The simultaneous presence of one platinum atom and one chlorine within the complex yields a characteristic isotopic pattern

for the cluster at m/z 610-614, easily distinguishable from any Pt-complex devoid of a chlorine atom, as in the case of the ion at m/z 574-578.

3.1 IRMPD spectroscopy of cis -[Pt(NH₃)₂(5'-dGMP)-H]⁺

During the last decade, IRMPD spectroscopy has been successfully applied to elucidate the structure of numerous ions from very simple fundamental species to (bio)molecular and composite cluster ions.^{12,14,31-50} We presently applied this approach to characterize the structure of cis -[Pt(NH₃)₂(5'-dGMP)-H]⁺. To this end, the whole isotopic cluster corresponding to the cis -[Pt(NH₃)₂(5'-dGMP)-H]⁺ ion (m/z 574-578) was isolated in the FT-ICR mass spectrometer, and submitted to IRMPD spectroscopy. The fragmentation of cis -[Pt(NH₃)₂(5'-dGMP-H)]⁺ upon irradiation by IR photons in resonance with an active vibrational mode yields four major fragment ions, namely a cluster at m/z 556-559, that includes two different species, corresponding to the loss of either water (m/z 556-558) or ammonia (m/z 557-559), respectively, a cluster at m/z 539-543 (the combined loss of NH₃ and H₂O), an ion m/z 522-526 resulting from the loss of two ammonia and one water molecules, and a cluster at m/z 441-445 due to loss of NH₃ together with the sugar residue (deoxyribosyl unit). (Figure S1 of the supporting information) In the last process, a complex where platinum is coordinated to ammonia, meta-phosphoric acid and a deprotonated guanine residue is formally obtained, namely [Pt(NH₃)(HPO₃)(G)-H]⁺. The formation of this particular fragment might suggest that in the cis -[Pt(NH₃)₂(5'-dGMP-H)]⁺ complex the 5'-dGMP ligand may act as a chelating agent coordinating the metallic centre with both guanine and an oxygen of the phosphate group, so giving a cyclic structure including Pt. This coordination is possible because platinum(II) in [Pt(NH₃)₂]²⁺ owns two free coordination sites at variance with [PtCl(NH₃)₂]⁺ forming the cis -[PtCl(NH₃)₂(5'-dGMP)]⁺ species. In our previous IRMPD study on cis -[PtCl(NH₃)₂(G)]⁺, similarly generated, we have found that the coordination site

of platinum is the N7 atom of guanine,⁷ confirming previous theoretical predictions on the interaction between cisplatin and guanine.^{51,52} So, it is reasonable to assume that one of the platination site is on the guanine residue. Another possible platination site could be an oxygen atom of the phosphoric moiety. Other minor fragment ions observed in the IRMPD experiments are the isotopic clusters associated with loss of water, ammonia and guanine (m/z 388-392). Finally, in the fragment detected at m/z 378-382, only the nucleobase of 5'-dGMP remains attached to $[\text{Pt}(\text{NH}_3)_2]^+$ as deprotonated guanine.

Aiming to obtain information about the structural features of the complex at m/z 574-578, IRMPD spectra recorded in both spectral regions were compared to the calculated IR spectra of candidate structures for the *cis*- $[\text{Pt}(\text{NH}_3)_2(5'\text{-dGMP-H})]^+$ complex. The various species are classified according to the platinum coordination scheme. **The lowest energies structures** obtained for this system are presented in Figure 2 together with their relative free energies at 298 K. A complete scheme with all the species investigated (showing relative free energies, coordination mode, ring puckering, orientation of the guanine unit, internal hydrogen bonding) is provided in the Supporting Information.

< **Figure 2** >

~~The first family of structures, namely **PtdGMP_A**, is associated with a bidentate interaction of the deprotonated phosphate group with the metal in the $(\text{NH}_3)_2\text{Pt}$ moiety. Though being a minimum, this structure is rather high in energy ($+167.9 \text{ kJ mol}^{-1}$). Bidentate coordination with both the deprotonated phosphate group and $\text{O}(3')\text{H}$ hydroxyl group (**PtdGMP_G**), reported in Figure S3 of the Supporting Information, does not result in a more stable species~~

~~(+177.0 kJ mol⁻¹ with respect to the global minimum). We also considered deprotonation of the O(3')H group. Interaction of platinum with O(3')⁻ and the phosphoryl (P=O) group (**PtdGMP_In**) gives rise to slightly more stable isomers. On the other hand, replacement of the phosphoryl group by the phosphohydroxyl (P-OH) induces a significant destabilization (**PtdGMP_H** in Figure S3; at +218.7 kJ mol⁻¹).~~

As shown by the relative free energies at 298 K reported in both Table S1 and Figure 2, the most stable structures (**PtdGMP_Dn**) correspond to macrochelate complexes where the *cis*-[Pt(NH₃)₂]²⁺ unit is coordinated to both the N7 position of guanine and the deprotonated oxygen of the phosphate group. Clearly, the interaction with N7 provides an important stabilization. All these forms are also characterized by a strong hydrogen bond established between one NH₃ ligand and the carbonyl group of guanine. The global minimum corresponds to the **PtdGMP_D5** *syn* structure. Slightly less stable is **PtdGMP_D6** (+2.6 kJ mol⁻¹) which shares with **PtdGMP_D5** the same characteristics except for the nucleobase orientation (*anti*). **PtdGMP_D4** only differs from **PtdGMP_D5** by the rotation of the phosphate group and lies at 3.6 kJ mol⁻¹ above the global minimum. These three forms all adopt a North sugar conformation (see Supporting Information for more details). **PtdGMP_D3** is also characterized by a *syn*-oriented guanine, but adopts a slightly less favorable ring puckering (C4'-endo/C3'-exo; +21.4 kJ mol⁻¹). Two other macrochelates were located, namely **PtdGMP_D1** and **PtdGMP_D2**, which are of similar stability as **PtdGMP_D3** but present a different nucleobase orientation (*anti*). Comparison of **PtdGMP_Dn** forms with the **PtdGMP_F** structure (+73.4 kJ mol⁻¹), in which the platinum ion interacts with both the deprotonated phosphate group and the carbonyl oxygen (O6) of guanine, further confirms the N7 centre of guanine as the most favourable coordination site.

A brief description of some other representative structure for the *cis*-[Pt(NH₃)₂(5'-dGMP-H)]⁺ complex is provide in the Supporting Information.

~~We also tried to optimize structures for which the *cis*-[Pt(NH₃)₂]²⁺ unit only interacts with N7. During optimization, these forms evolve either by proton transfer between an ammonia group and the deprotonated phosphate (**PtdGMP_Cn**) or towards a bidentate interaction involving both N7 and the phosphate (**PtdGMP_D** forms). Finally, we also envisaged coordination onto the N3 position of guanine. The most stable structure found and reported in this paper (**PtdGMP_J1**, Figure 2) implies a C1'exo ring puckering, which, associated with the *syn* orientation of the guanine residue, allows the simultaneous interaction with the deprotonated phosphate. This structure is located at 91.2 kJ mol⁻¹ above the global minimum.~~

The IRMPD spectra of *cis*-[Pt(NH₃)₂(5'-dGMP-H)]⁺ recorded in the 700–1900 and 2800–3800 cm⁻¹ spectral range are reported in the lower panel of Figure 3, together with the calculated IR spectra of some exemplary species among the ones displayed in Figure 2.

< Figure 3 >

In the fingerprint domain, the IRMPD spectrum of *cis*-[Pt(NH₃)₂(5'-dGMP-H)]⁺ presents distinct features at 1021, 1095, 1283, 1582 1627 and 1701 cm⁻¹ (figure **3a**). Other weaker bands are found at 902, 931, 1169, 1198, 1367 and 1516 cm⁻¹. In the X-H (X = C, N, O) stretching range, the IRMPD spectrum of *cis*-[Pt(NH₃)₂(5'-dGMP-H)]⁺ shows two sharp bands at 3422 and 3672 cm⁻¹ and a broad band at 3439-3453 cm⁻¹. A few weaker absorptions are detected at ca. 2919-2984, 3156, 3381 and 3557 cm⁻¹. The calculated spectra of **PtdGMP_D4-6** provide the best fit with the experimental spectrum (Figure 3). Thus, the vibrational modes of *cis*-[Pt(NH₃)₂(5'-dGMP-H)]⁺ can be assigned as described in Table 1,

which lists the experimental IRMPD features together with the calculated IR bands of the global minimum **PtdGMP_D5**. Focusing on the main absorptions in the fingerprint range, the pronounced and broad experimental band at 1021 cm^{-1} can be assigned to the feature centered at 993 cm^{-1} comprising several vibrational modes, calculated at $976, 991, 994,$ and 1019 cm^{-1} associated to stretches of the O–P=O–Pt unit, PO–H bending, and to the furanolic ring breathing. The feature at 1283 cm^{-1} can be assigned to two active modes, namely the P=O stretching mode at 1276 cm^{-1} and the umbrella mode of NH_3 not involved in hydrogen bonding with the carbonyl oxygen (O6) of the guanine, at 1287 cm^{-1} . The three major features at $1582, 1627$ and 1701 cm^{-1} are the characteristic signature of the coordination of the *cis*- $[\text{Pt}(\text{NH}_3)_2]^{2+}$ moiety onto the N7 position of guanine, as previously observed for the *cis*- $[\text{PtCl}(\text{NH}_3)_2(\text{G})]^+$ complex.⁷ Indeed, as shown in Figure **3(b-e)**, these three features are present in all computed spectra for **PtdGMP_Dn** ($n=1, 4, 5, 6$), in which one of the platination site by the *cis*- $[\text{Pt}(\text{NH}_3)_2]^{2+}$ unit is the nitrogen N7 of guanine. The first band at 1582 cm^{-1} can be assigned to NH_2 scissoring combined with the stretching of several purine ring bonds. The second feature can be attributed to the combination of different NH_2 scissoring modes, and the last one to the CO stretch of guanine. These modes are computed at $1582, 1635$ and 1699 cm^{-1} respectively, for **PtdGMP_D5**. The relatively low wavenumber associated with the carbonyl stretch is explained by the strong hydrogen bond established between the carbonyl oxygen and a hydrogen atom of one ammonia ligand of the $[\text{Pt}(\text{NH}_3)_2]^{2+}$ unit, favored when platinum is bound to the N7 position. This strong hydrogen bond decreases the force constant of the C=O bond causing a redshift in the absorption frequency with respect to an unperturbed C=O bond. In **PtdGMP_F** and **PtdGMP_B2** (Figure S4 of the supporting information) where the metal interacts directly with the guanine carbonyl group, the CO stretch is calculated at 1449 and 1512 cm^{-1} respectively, indicative of a

strongly weakened bond. Note that the very intense feature (1853 cm^{-1}) associated with the N-H stretch in the spectrum of **PtdGMP_B2** is not observed experimentally, disproving any contribution of this particular isomer.

Now considering the X-H stretch region, the calculated spectra do not reproduce the experimental data (figure 3a') quite well. In particular, one notices the absence of few small absorptions pertaining to the symmetric and antisymmetric stretching of the NH_3 ligands. These modes tend to give broad absorptions and it is possible that, because of their low IR intensity, they fall below the detection threshold of our apparatus. However, these modes are common in the IR spectra of most of the species concerned, and consequently are not so important for the purpose of structural recognition. On the other hand, the IRMPD spectrum shows important features which confirm the structural assessments deduced from fingerprint region. The major band at 3672 cm^{-1} can be assigned to the PO-H and O(3')-H stretching modes computed at 3673.6 and 3674.1 cm^{-1} , respectively, for **PtdGMP_D5**. The N1-H stretching mode appears at 3422 cm^{-1} and the broad feature at $3440\text{-}3453\text{ cm}^{-1}$ can be assigned to the symmetric NH_2 stretching mode, that are expected at 3424 and 3446 cm^{-1} , respectively, for **PtdGMP_D5**. The small, broad feature with a maximum at 2984 cm^{-1} is important to characterize the complex at m/z 574-578, formed in aqueous solution. It is reproduced only in the calculated spectra of **PtdGMP_D4-6**, and therefore is highly diagnostic. It is due to the stretch of the N-H bond involved in the strong hydrogen bond between the ammonia ligand of the $\text{cis-}[\text{Pt}(\text{NH}_3)_2]^{2+}$ unit and the carbonyl oxygen of the guanine, and calculated at 2968 cm^{-1} . OPO experiments may also provide some information about the nucleobase orientation within the complex. As can be observed from the calculated spectra reported in Figure 3, the position of the PO-H stretch is the same for all the species considered, while that of the OH hydroxyl changes. Within the **PtdGMP_Dn** family, the

O(3')-H stretch and the PO-H stretch present strictly close frequencies only in conformers **D5** and **D4**, the ones characterized by a *syn* configuration (figure **3(b',d')**).

In summary, IRMPD experiments in both spectral ranges unambiguously show that gaseous *cis*-[Pt(NH₃)₂(5'-dGMP-H)]⁺ ions exhibit a macrochelate structure resulting from the simultaneous interaction of the metal with both the N7 atom of guanine and the phosphate group. Their structure is therefore similar to those characterized in solution by NMR spectroscopy.^{8,9} Note that unlike what was postulated from calculations in these studies, the best agreement is presently obtained for macrochelates having a North sugar conformation (**PtdGMP_D4** and **PtdGMP_D5**) and a *syn* orientation of guanine.

3.2 IRMPD spectroscopy of *cis*-[PtCl(NH₃)₂(5'-dGMP)]⁺

As in the case of the *cis*-[Pt(NH₃)₂(5'-dGMP-H)]⁺ complex, the whole isotopic pattern at *m/z* 610-614 corresponding to the *cis*-[PtCl(NH₃)₂(5'-dGMP)]⁺ complex was isolated in the cell of the mass spectrometer in order to be submitted to IRMPD spectroscopy. Photofragmentation of *cis*-[PtCl(NH₃)₂(5'-dGMP)]⁺ occurs along three different channels (Supporting Information, Figure S2). The main one is associated with loss of HCl giving rise to the *cis*-[Pt(NH₃)₂(5'-dGMP-H)]⁺ complex (cluster at *m/z* 574-578), which in turn gives four further fragments at *m/z* 556-559, 539-543, 522-526, 441-445, as already discussed in the previous section (*vide supra*). The second channel corresponds to the loss of ammonia, to generate the cluster at *m/z* 593-597. The last fragmentation channel involves the cleavage of the *N*-glycosidic bond, presumably leading to the *cis*-[PtCl(NH₃)₂(G)]⁺ complex (cluster at *m/z* 414-418), which in turn expels ammonia to yield *cis*-[PtCl(NH₃)(G)]⁺ at *m/z* 397-401. These two last fragment ions suggest that the preferred site of platination on 5'-dGMP remains the guanine residue.

This last photofragmentation channel and the calculations carried out for the *cis*-[Pt(NH₃)₂(5'-dGMP)-H]⁺ complex, which demonstrate the greater affinity of *cis*-[Pt(NH₃)₂]⁺ for the nucleobase rather than for the phosphate group, led us to limit our computational survey to structures just involving platination onto guanine. A detailed description (coordination site, orientation of the base, configuration of the sugar ring, and intramolecular hydrogen bonds) of all the species investigated is given in the Supporting Information. As shown in Figure S4, most of the geometries are characterized by bonding of platinum onto the N7 position of guanine. For the sake of comparison, bonding of Pt with N3 has also been considered, yielding the **PtClIdGMP_Fn** family of isomers. Though characterized as local minima, these species are much less stable than the the N7-bonded structures.

Optimized geometries of representative structures of *cis*-[PtCl(NH₃)₂(5'-dGMP)]⁺ are gathered in Figure 4, together with their relative free energies at 298K. This last photofragmentation channel and the calculations carried out for the *cis*-[Pt(NH₃)₂(5'-dGMP-H)]⁺ complex, which demonstrate the greater affinity of *cis*-[Pt(NH₃)₂]⁺ for the nucleobase rather than for the phosphate group, led us to limit our computational survey to structures just involving platination onto guanine. A detailed description (coordination site, orientation of the base, configuration of the sugar ring, and intramolecular hydrogen bonds) of all the species investigated is given in the Supporting Information. As shown in Figure S5, most of the geometries are characterized by bonding of platinum onto the N7 position of guanine. Optimized geometries of representative structures of *cis*-[PtCl(NH₃)₂(5'-dGMP)]⁺ are gathered in Figure 4, together with their relative free energies at 298K.

< **Figure 4** >

The three most stable forms (**PtClIdGMP_En**, **PtClIdGMP_B2**) share similar characteristics, which can be described as follows: coordination of *cis*-[PtCl(NH₃)₂]⁺ onto the N7 site of guanine, North sugar conformation, and the same ammonia ligand engaged in two hydrogen bonds, one with an oxygen of the phosphate group and the second one with the carbonyl oxygen (O6) of guanine. The global minimum is **PtClIdGMP_E1**, where a third hydrogen bond between the phosphate group and the oxygen atom of the deoxyribose moiety (O'1) can be also envisaged. This latter hydrogen bond provides additional stabilization (by ca. 13 kJ mol⁻¹). Comparison of **PtClIdGMP_E2** and **PtClIdGMP_B2** shows that the nucleobase orientation has no noticeable effect on the stability for a given configuration.

In all the other configurations investigated, the ammonia ligand is involved in a single hydrogen bond with O6. Slightly less stable are the **PtClIdGMP_C1** and **PtClIdGMP_C2** structures. These forms are also folded thanks to the presence of a hydrogen bond between the phosphate group and the amino group of guanine. Such hydrogen bonding requires the guanine to adopt a *syn* orientation, and has already been experimentally observed for deprotonated 5'-dGMP.^{32,53} A brief description of some other representative structure for *cis*-[PtCl(NH₃)₂(5'-dGMP)]⁺ complex is provided in the Supporting Information.

~~**PtClIdGMP_A1** and **PtClIdGMP_A2** are characterized by a weak hydrogen bond between one hydrogen of the phosphate group and the chlorine ligand. These two latter structures are less stable than **PtClIdGMP_E1** by about 30 kJ mol⁻¹. Finally, the least stable optimized forms are **PtClIdGMP_D1** and **PtClIdGMP_D2**. In these species, the phosphate group is hydrogen bonded to the O3' hydroxyl group and no longer interacts with the *cis*-[PtCl(NH₃)₂]⁺ moiety, resulting in a significant destabilization (+57 kJ mol⁻¹ with the respect to the global minimum).~~

The IRMPD spectra of *cis*-[PtCl(NH₃)₂(5'-dGMP)]⁺ ions in both spectral ranges, namely 700-1900 cm⁻¹ and 2850-3700 cm⁻¹, are plotted in Figures **5a** and **5a'**, respectively, together with the vibrational spectra computed for the stable species displayed in Figure 5.

< **Figure 5** >

In the fingerprint region the experimental spectrum of *cis*-[PtCl(NH₃)₂(5'-dGMP)]⁺ shows eight pronounced features at 927, 964, 1095, 1275, 1300, 1582, 1632 and 1725 cm⁻¹, and other minor bands at 1009, 1038, 1156, 1214, 1422 and 1533 cm⁻¹. Comparing this experimental spectrum with calculated IR spectra (fig **5b-e**), the best agreement is obtained with either **PtClIdGMP_En** (n = 1,2) structures. The experimental IRMPD features are listed in Table 2 together with the IR bands calculated for **PtClIdGMP_E2**. As previously observed for *cis*-[Pt(NH₃)₂(5'-dGMP-H)]⁺ (*vide supra*) and *cis*-[PtCl(NH₃)₂(G)]⁺ complexes,⁵⁴ the IRMPD spectrum of *cis*-[PtCl(NH₃)₂(5'-dGMP)]⁺ presents the three characteristic strong features (here at 1582, 1632 and 1725 cm⁻¹), attributed to the NH₂ scissoring, NH₃ and N'H₃ scissoring modes, and the C6=O stretching modes, and computed at 1579, 1635 and 1714 cm⁻¹, respectively. Again, the C=O stretch is red-shifted with respect to an unperturbed C=O stretching mode. On the other hand, it appears slightly blue-shifted when compared to the frequency of this mode for both *cis*-[Pt(NH₃)₂(5'-dGMP-H)]⁺ (1701 cm⁻¹) and *cis*-[PtCl(NH₃)₂(G)]⁺ (1718 cm⁻¹) ions. This point appears even more clearly by comparing the energy gap between the two adjacent bands corresponding to NH₂ scissoring and C=O stretch. This gap is about 74 cm⁻¹ for *cis*-[Pt(NH₃)₂(5'-dGMP-H)]⁺, 81 cm⁻¹ for *cis*-[PtCl(NH₃)₂(G)]⁺ and increases up to 93 cm⁻¹ for *cis*-[PtCl(NH₃)₂(5'-dGMP)]⁺. This effect can be interpreted by the fact that in the latter complex, the ammonia ligand is involved in two different hydrogen

bonds, as shown in Figure 4 (**PtClIdGMP_En** and **PtClIdGMP_B2**), resulting in the weakening in the $\text{H}_2\text{N}-\text{H}\cdots\text{O}=\text{C}$ hydrogen bond. Consequently, the double bond character of $\text{C6}=\text{O}$ decreases to a lesser extent, and the carbonyl stretch is measured at higher energy with respect to the other complexes. This effect is also illustrated by Figure S6 (Supporting Information), which compares the experimental IRMPD spectra of both $\text{cis}-[\text{Pt}(\text{NH}_3)_2(5'\text{-dGMP}-\text{H})]^+$ and $\text{cis}-[\text{PtCl}(\text{NH}_3)_2(5'\text{-dGMP})]^+$ in the fingerprint region. Conversely, the $\text{C6}=\text{O}$ stretching mode is expected at 1693 cm^{-1} for **PtClIdGMP_C1** (Figure 5), in which the ammonia ligand is solely hydrogen-bonded with O6.

The broad feature around 1290 cm^{-1} comprises two peaks at 1275 and 1300 cm^{-1} , and a shoulder at 1250 cm^{-1} . According to our calculations, the first one can be assigned to the calculated band centered at 1290 cm^{-1} , formed by the convolution of three different vibrational modes, namely $\text{P}=\text{O}$ stretching modes at 1285 and 1292 cm^{-1} , and the umbrella bending mode of the $\text{N}'\text{H}_3$ ligand (not involved in the hydrogen bonding) at 1289 cm^{-1} . The second feature at 1300 cm^{-1} may correspond to the convolution of two vibrational modes, $\text{N1}-\text{H}$ bending and NH_3 umbrella modes, computed at 1319 and $\text{ca } 1322\text{ cm}^{-1}$, respectively. The feature at 1095 cm^{-1} is also found in the IRMPD spectrum of $\text{cis}-[\text{Pt}(\text{NH}_3)_2(5'\text{-dGMP}-\text{H})]^+$ and may be attributed to both $\text{C}'-\text{H}$ and $\text{C}'-\text{OH}$ bending modes and the $\text{P}-\text{OC}$ stretching mode. In agreement with this assignment, this band is not present in the experimental IRMPD spectrum of $\text{cis}-[\text{PtCl}(\text{NH}_3)_2(\text{G})]^+$.⁵⁴ Conversely, the partially-resolved bands with the two maxima at 927 and 964 cm^{-1} are not detected for the $\text{cis}-[\text{Pt}(\text{NH}_3)_2(5'\text{-dGMP})-\text{H}]^+$ adduct (Figure 2), and can be interpreted as the convolution of the of $\text{P}-\text{OH}$ stretching and bending modes calculated at $909-910\text{ cm}^{-1}$ for the former, and the stretching $\text{P}-\text{OC}$ mode combined with the furanose ring breathing expected at 959 cm^{-1} for the latter.

The *cis*-[PtCl(NH₃)₂(5'-dGMP)]⁺ ions have also been examined in the X-H (X = C,N,O) stretching region from 2800 to 3800 cm⁻¹. As reported in Figure 5a', *cis*-[PtCl(NH₃)₂(5'-dGMP)]⁺ presents three major absorptions, observed at 3427, 3450 and 3668 cm⁻¹. Other weaker but still significant features are detected at 3356, 3386, and 3558 cm⁻¹. Based on a comparison with the calculated IR spectra reported in Figure 5b'-e', quite a good agreement is found between the experimental spectrum and the IR spectrum of conformer **PtCldGMP_E2** and also with **PtCldGMP_B2**. The main feature at 3668 cm⁻¹ can be assigned to the convolution of three active modes combining P-OH and the O3'-H stretches (computed at 3667 and 3670 cm⁻¹). The two absorptions at 3450 cm⁻¹ and 3558 cm⁻¹ are due to the symmetric and asymmetric stretches of NH₂, expected at 3446 and 3560 cm⁻¹, respectively, for **PtCldGMP_E2**. The band at 3427 cm⁻¹ corresponds to the N1-H stretching mode expected at 3425 cm⁻¹. The two weak absorptions at 3356 and 3386 cm⁻¹ are consistent with the asymmetric stretching modes of the N³H₃ ligand, estimated at 3359 and 3395 cm⁻¹, respectively.

Furthermore, the IRMPD spectrum of *cis*-[PtCl(NH₃)₂(5'-dGMP)]⁺ shows two broad absorptions, the most important between 3116 and 3219 cm⁻¹, and a second one at ca. 3270 cm⁻¹ (from 3227 to 3294 cm⁻¹). The more pronounced one can be assigned to the stretch of N-H bonds involved in hydrogen bonding. Experimentally, the IRMPD feature for this kind of stretching mode was often found quite weak and also red-shifted with respect to the calculated position (as was observed for example for water solvated clusters⁵⁵, solvated amino acids⁵⁶ or nucleobases^{57,58} and lactic ester derivatives⁵⁹) even if their predicted intensities are very high. The most common explanation lies in the anharmonicity of this mode and the ensuing low IRMPD efficiency. Within this broad absorption, two maxima may be discerned at 3144 and at 3177 cm⁻¹, that may be assigned to symmetric and asymmetric N-H stretching mode of the

two NH bonds of the ammonia ligand involved in two hydrogen bond interactions, calculated at 3146 and 3205 cm^{-1} , respectively. As observed in the fingerprint region, the simultaneous involvement in these two hydrogen bonds by the same ammonia ligand decreases the strength of these interactions with respect to an otherwise single hydrogen bond. Consequently, the covalent N-H bonds involved in hydrogen bonding are stronger than the one observed in the case of *cis*-[PtCl(NH₃)₂(G)]⁺ and *cis*-[Pt(NH₃)₂(5'-dGMP-H)]⁺. Therefore, this mode is active at relatively higher frequency, calculated to be half-way between a free N-H bond (typically 3340 cm^{-1}) and a N-H bond in a single and strong hydrogen bond (3054 cm^{-1}), as previously observed in the case of *cis*-[PtCl(NH₃)₂(G)]⁺.⁷ It is worth noting that all other vibrational modes common to both *cis*-[PtCl(NH₃)₂(G)]⁺, *cis*-[Pt(NH₃)₂(5'-dGMP-H)]⁺ and *cis*-[PtCl(NH₃)₂(5'-dGMP)]⁺ fall exactly at the same position as reported in Figure S7 (Supporting Information). Interestingly, the PO-H stretch involved in a hydrogen bond with the furanolic oxygen, expected at 3327 cm^{-1} and pertaining only to **PtCldGMP_E1**, is missing in our experimental spectrum. Possibly, the second tiny broad absorption found between 3227 and 3294 cm^{-1} could be associated to this specific mode. However, the calculated spectrum of **PtCldGMP_E2** presents also a small absorption at 3269 cm^{-1} corresponding to the asymmetric N-H stretch of N'H₃. In either circumstances, it may be safely stated that *cis*-[PtCl(NH₃)₂(5'-dGMP)]⁺ ions generated in solution and analyzed in the gas phase exhibit a chelate structure consistent with the geometry of **PtCldGMP_E2** while **PtCldGMP_E1** may also contribute, albeit to a minor extent.

In summary, *cis*-[PtCl(NH₃)₂(5'-dGMP)]⁺ ions generated in the gas phase by ESI ionization are characterized by a monodentate interaction of the Platinum onto the N7 position of guanine, like already observed in the gas phase for guanine,⁷ or in solution for 5'GMP.^{10,11}

The structures characterized by our IRMPD experiments turn to be rather compact due to the involvement of the same ammoniac ligand in two hydrogen bonds.

Conclusions

The purpose of this study is to provide an accurate characterization of cis -[Pt(NH₃)₂(5'-dGMP-H)]⁺ and cis -[PtCl(NH₃)₂(5'-dGMP)]⁺ taken as models of the monofunctional adduct between cisplatin and DNA, using IRMPD spectroscopy. Mass spectrometry has the ability to isolate the ions of interest to be submitted to the IR characterization, allowing the study of transient or highly reactive ions such as cis -[PtCl(NH₃)₂(5'-dGMP)]⁺. The present study has confirmed a macrochelate structure for the cis -[Pt(NH₃)₂(5'-dGMP-H)]⁺ ion where the Pt is coordinated both to the N7 position of guanine and to the deprotonated oxygen of the phosphate group, with a North sugar conformation as previously predicted by NMR spectroscopy^{8,9}, but at variance with what postulated before the better agreement seems to be with a *syn* base orientation. In the cis -[PtCl(NH₃)₂(5'-dGMP)]⁺ where platinum ion allows a only one coordination site to 5'-dGMP, the coordination is direct only onto the N7 position of the guanine, with one of the two ammonia ligands involved in two hydrogen bonds, one with an oxygen of the phosphate group and the second one with the carbonyl oxygen (O6) of guanine. This motif causes a somewhat low strength in both hydrogen bonds, as reflected in the IRMPD spectra: the carbonyl stretch is active at higher energy than in cis -[Pt(NH₃)₂(5'-dGMP-H)]⁺ and the stretch of the N-H bond involved in the hydrogen bond appears to be active at a frequency in half-way between that of a free N-H and that of a N-H involved in a strong hydrogen bond.

Acknowledgements

The authors wish to thank the CLIO team (J. M. Ortega, C. Six, G. Perilhous, J. P. Berthet) as well as P. Maître, V. Steinmetz and A. Di Marzio for their support during the experiments. JYS is grateful to the computational centre of the Universidad Autonoma de Madrid for computing facilities. Financial support has been provided by the Italian MIUR (Prin project 2009W2W4YF_004) and by the European Union (project IC019-12 entitled ‘The interaction of cisplatin with nucleic acids: an approach by IRMPD spectroscopy. II’)

Supporting Information Available

Detailed photofragmentation mass spectra of ions under examination; all computed structures for *cis*-[Pt(NH₃)₂Cl(5'-dGMP)]⁺ and *cis*-[Pt(NH₃)₂(5'-dGMP-H)]⁺ are gathered into a supporting information. This material is available free of charge via the Internet at <http://pubs.acs.org/>

Table 1: Experimental spectrum of the *cis*-[Pt(NH₃)₂(5'-dGMP-H)]⁺ complex and computed vibrational modes for the **PtdGMP_D5** isomer.

Wavenumber (cm ⁻¹)		Vibrational mode ^b
IRMPD	Calculated ^a	
Fingerprint region (FEL)		
902	855 (103)	β N8H + ν POH
	861 (90)	ν POH
	881 (81)	NH ₃ Twist
	893 (124)	ν P-OC5' + Furanosic ring breathing
931	935 (96)	Furanosic ring breathing
1021	976 (206)	ν O-P=O-Pt + ν P-O5'
	991 (325)	ν P=O-Pt + β POH
	994 (107)	Furanosic ring breathing
	1019 (71)	Furanosic ring breathing + C(5')H ₂ Rock
1095	1068 (125)	NH ₂ Rock + ν C3'OH
	1071 (82)	NH ₂ Rock
	1085 (138)	Furanosic ring breathing + C(5')H ₂ Rock
	1098 (44)	ν C4'C5'
1169	1153 (78)	ν C6N1 + β C8H
1198	1188 (96)	ν C1'N9
	1224 (132)	ν C8N9 + β C'H
1283	1276 (164)	ν P=O
	1287 (120)	N'H ₃ umbrella
1320	1322 (125)	β N1'H
	1329 (44)	β N1'H + guanine ring breathing
1367	1350 (78)	NH ₃ umbrella
1516	1525 (65)	β C8H + guanine ring breathing
1582	1563 (69)	ν C4-C5
	1582 (333)	δ NH ₂ Sciss + ν C4-N3
1627	1635 (951)	β NH ₂ Sciss of NH ₂
	1659 (115)	β NH ₂ Sciss of NH ₃
1701	1699 (594)	ν C=O
X-H stretch region (OPO)		
2919-2984	2915 (19)	ν C(5')H ₂ sym
	2938 (23)	ν C4'H + ν C(2')H ₂ sym
	2968 (602)	ν N-H of NH ₃ ⁺ O=C6
3156	3168 (26)	ν C8H
-	3262 (26)	ν N'H ₃ sym
-	3337 (47)	ν NH ₃ asym
-	3358 (59)	ν N'H ₃ asym
3381	3395 (31)	ν N'H ₃ asym
	3396 (38)	ν NH ₃ asym
3422	3424 (63)	ν N1-H
3440-3453	3446 (203)	ν NH ₂ sym
~ 3557	3560 (72)	ν NH ₂ asym
3672	3674 (165)	ν OH Phos
	3674 (51)	ν O(3')H

^(a) Calculated vibrational modes at the B3LYP/6-311G** level of theory. The computed intensities (km mol⁻¹) are given in parenthesis. In the fingerprint region, bands with intensity lower than 40 km mol⁻¹ are not included.

^(b) β = bending; ν = stretching, Wag = wagging, Rock = rocking, Sciss = scissoring. NH_3 denotes the ammonia interacting with the carbonyl group, $\text{N}'\text{H}_3$ denotes the other ammonia ligand.

Table 2: Experimental spectrum of the *cis*-[PtCl(NH₃)₂(5'-dGMP)]⁺ complex and computed vibrational modes for the **PtCl dGMP_E2** isomer

Wavenumber (cm ⁻¹)		Vibrational mode ^b
IRMPD	Calculated ^a	
Fingerprint region (FEL)		
927	909 (274)	ν POH + β POH phosphate
	910 (191)	ν P=OH + β POH phosphate (both)
964	959 (105)	Furanosic ring breathing + ν P-OC
	982 (61)	ν P-OC + Furanosic ring breathing
1009	1017 (74)	β POH + ν P-O
1038	1043 (114)	ν POC + Furanosic ring breathing β POH
	1056 (115)	ν P-OC + Furanosic ring breathing β POH
1095	1102 (172)	β C4'-H + ν β C3'-OH + ν P-OC
	1115 (137)	Furanosic ring breathing; β C3'O-H ν P-OC
1156	1137 (40)	ν C4'-C5' ν P-OC
	1142 (63)	Guanine ring breathing + β C8-H
1214	1192 (52)	ν N9-C1' + Guanine ring breathing + β C8-H
	1224 (87)	ν N9-C1' + β C8-H + β C3'O-H
1275-1300	1285 (129)	ν P=O + Twisting C5'H2
	1289 (115)	N'H ₃ umbrella
	1292 (309)	ν P=O + C(5')H ₂ Twist C5'H2 Twist
	1319 (126)	NH ₃ umbrella + β N1-H
	1322 (81)	NH ₃ umbrella
1422	1401 (41)	β C'1-H + Guanine ring breathing
1533	1526 (79)	Guanine ring breathing + β C8-H
1582	1563 (71)	β sciss NH ₂ + ν C4-C5
	1579 (350)	β sciss NH ₂
1632	1620 (131)	β NH ₂ rock of NH ₃
	1633 (418)	β sciss NH ₂ + β NH ₂ rock N'H ₃
	1635 (446)	β NH ₂ sciss of NH ₂ and NH ₃
	1664 (43)	β NH ₂ sciss of NH ₃
1725	1714 (534)	ν C=O
X-H stretch region (OPO)		
3116-3210 (3144-3172)	3146 (358)	ν NH ₃ sym double H Bonded PO and C6O
	3205 (400)	ν NH ₃ asym double H Bonded PO and C6O
(3227-3294) 3270	3269 (17)	ν N'H ₃ sym
3356	3359 (46)	ν N'H ₃ asym
3386	3394 (39)	ν N'H ₃ asym (2H)
	3396 (37)	ν NH ₃ not involved in H bonding
3427	3425 (58)	ν N1H
3450	3446 (193)	ν NH ₂ sym
3558	3560 (69)	ν NH ₂ asym
3668	3667 (137)	ν POH asym (both)
	3670 (126)	ν C3'O-H and + ν POH sym (both)
	3670 (119)	ν POH sym (both) and+ ν C3'O-H

^(a) Vibrational modes Calculated at the B3LYP/6-311G** level of theory. The computed intensities (km mol^{-1}) are given in parenthesis. In the fingerprint region, bands with intensity lower than 40 km mol^{-1} are not included.

^(b) β = bending; ν = stretching, Wag = wagging, Rock = rocking, Sciss = scissoring. NH_3 denotes the ammonia interacting with the carbonyl group, $\text{N}'\text{H}_3$ denotes the ammonia located near the chlorine atom.

Captions for Figures

Figure 1. Structure of 2'-deoxyguanosine-5'-monophosphate (here with an *anti* configuration and a North sugar conformation). C are in dark grey, N in blue, O in red, P in magenta and H in light grey.

Figure 2. Geometries and relative free energies (kJ mol^{-1}) for the more stable structures of $\text{cis-}[\text{Pt}(\text{NH}_3)_2(5'\text{-dGMP-H})]^+$ ions calculated at the B3LYP/6-311G** level. Distances are in Å.

Figure 3. Figure 3. Experimental IRMPD spectrum of the $\text{cis-}[\text{Pt}(\text{NH}_3)_2(5'\text{-dGMP-H})]^+$ complex (bottom) in both fingerprint (**a**) and X-H (X = C,N,O) stretch (**a'**) regions, compared with the IR spectra of structures reported in Figure 2 computed at the B3LYP/6-311G** level. See text for details

Figure 4. Geometries and relative free energies (kJ mol^{-1}) of representative $\text{cis-}[\text{PtCl}(\text{NH}_3)_2(5'\text{-dGMP})]^+$ structures calculated at the B3LYP/6-311G** level. Distances are in Å.

Figure 5. Experimental IRMPD spectrum of the $\text{cis-}[\text{PtCl}(\text{NH}_3)_2(5'\text{-dGMP})]^+$ complex (bottom) in both fingerprint (**a**) and X-H (X = C,N,O) stretch (**a'**) region compared to IR spectra of representative structures computed at the B3LYP/ 6-311G** level. See text for details.

Figures

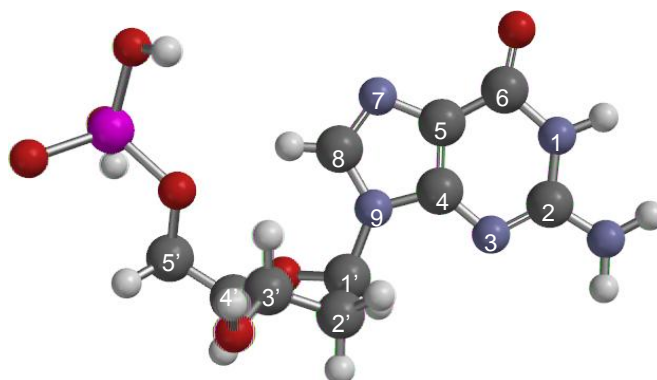


Figure 1. Structure of 2'-deoxyguanosine-5'-monophosphate (here with an *anti* configuration and a North sugar conformation). C are in dark grey, N in blue, O in red, P in magenta and H in light grey.

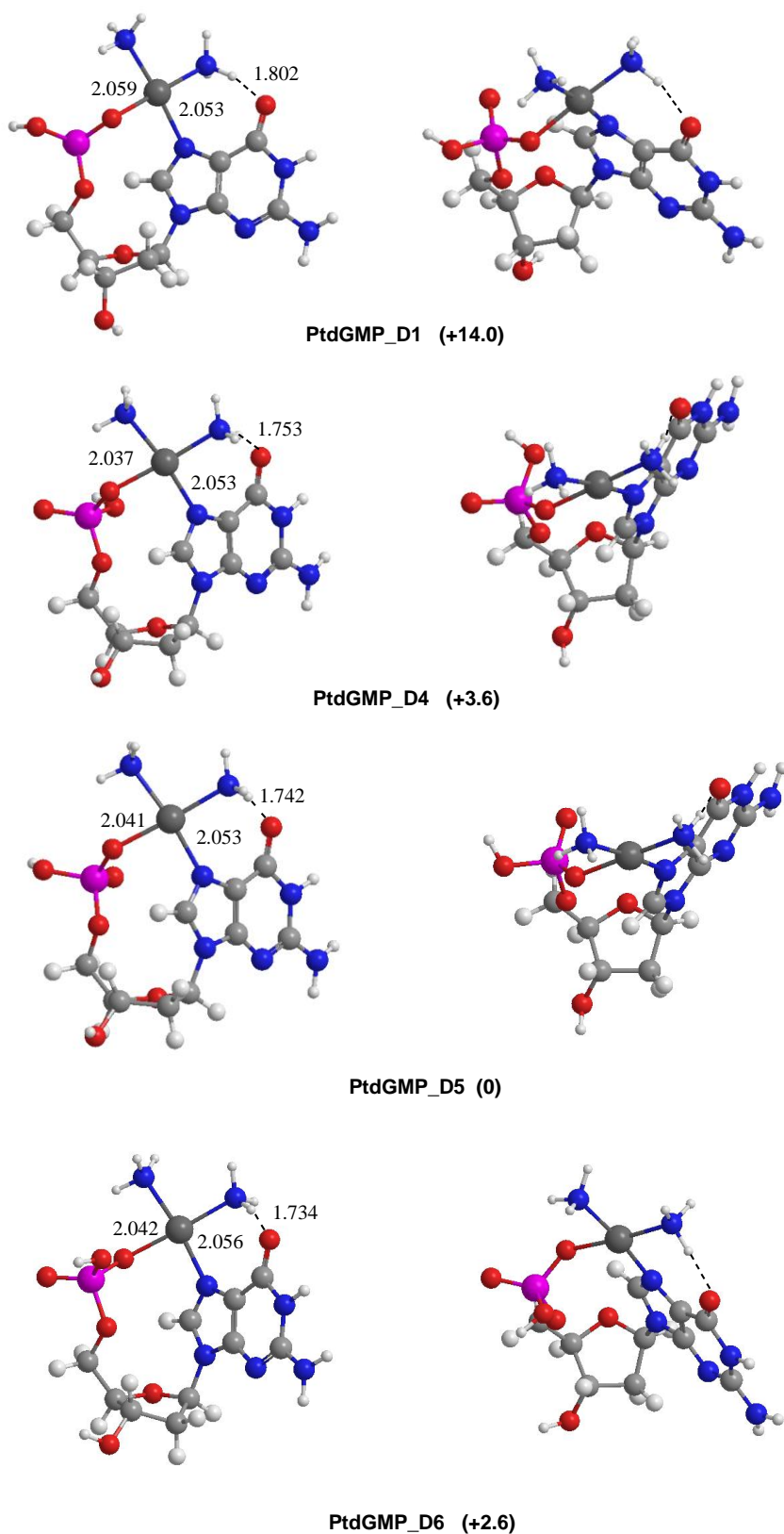


Figure 2. Geometries and relative free energies (kJ mol^{-1}) for the most stable structures of *cis*- $[\text{Pt}(\text{NH}_3)_2(5' \text{-dGMP-H})]^+$ ions calculated at the B3LYP/6-311G** level. Distances are in Å.

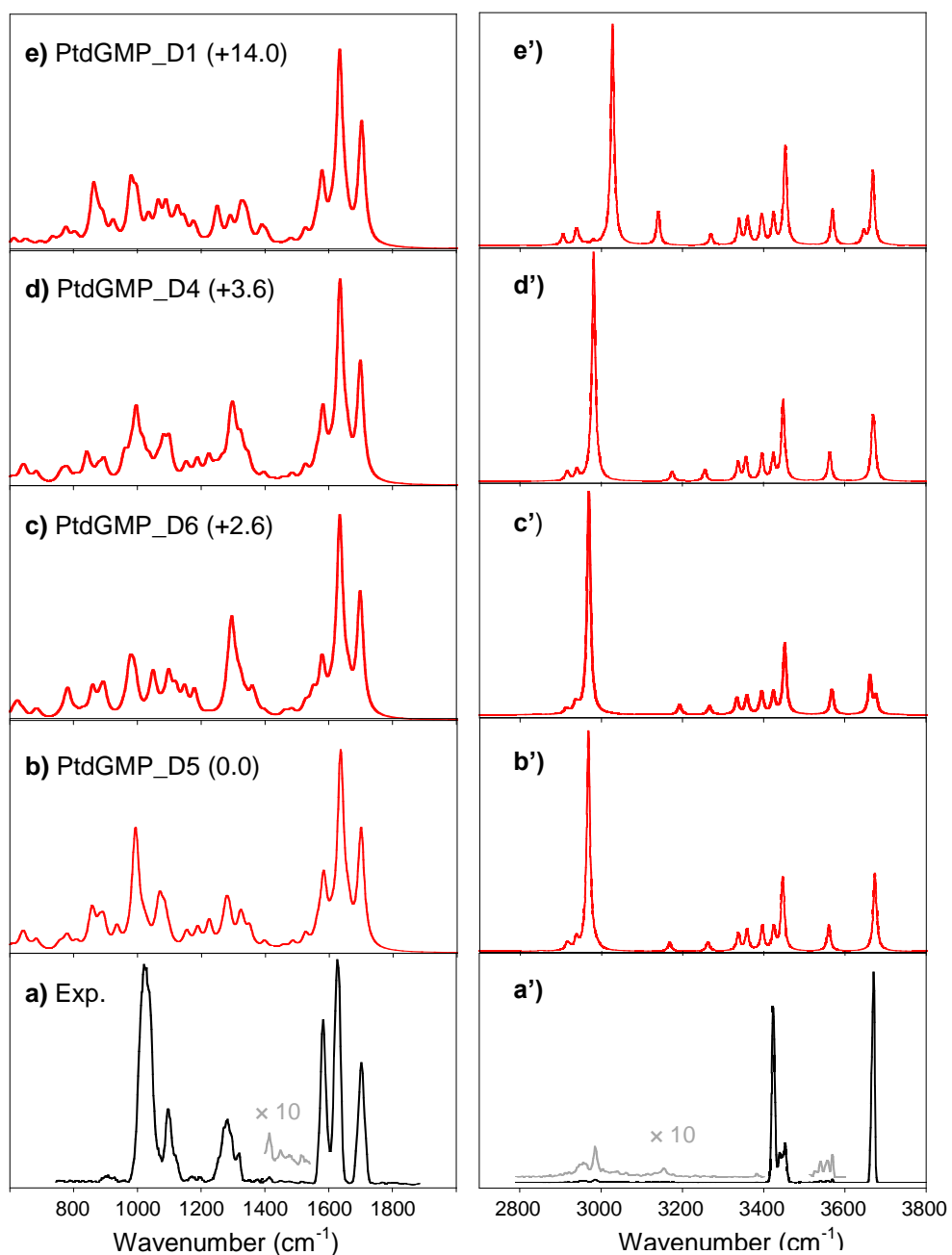


Figure 3. Experimental IRMPD spectrum of the cis - $[Pt(NH_3)_2(5'-dGMP-H)]^+$ complex (bottom) in both fingerprint (a) and X-H (X = C,N,O) stretch (a') regions, compared with the IR spectra of structures reported in Figure 2 computed at the B3LYP/6-311G** level. See text for details

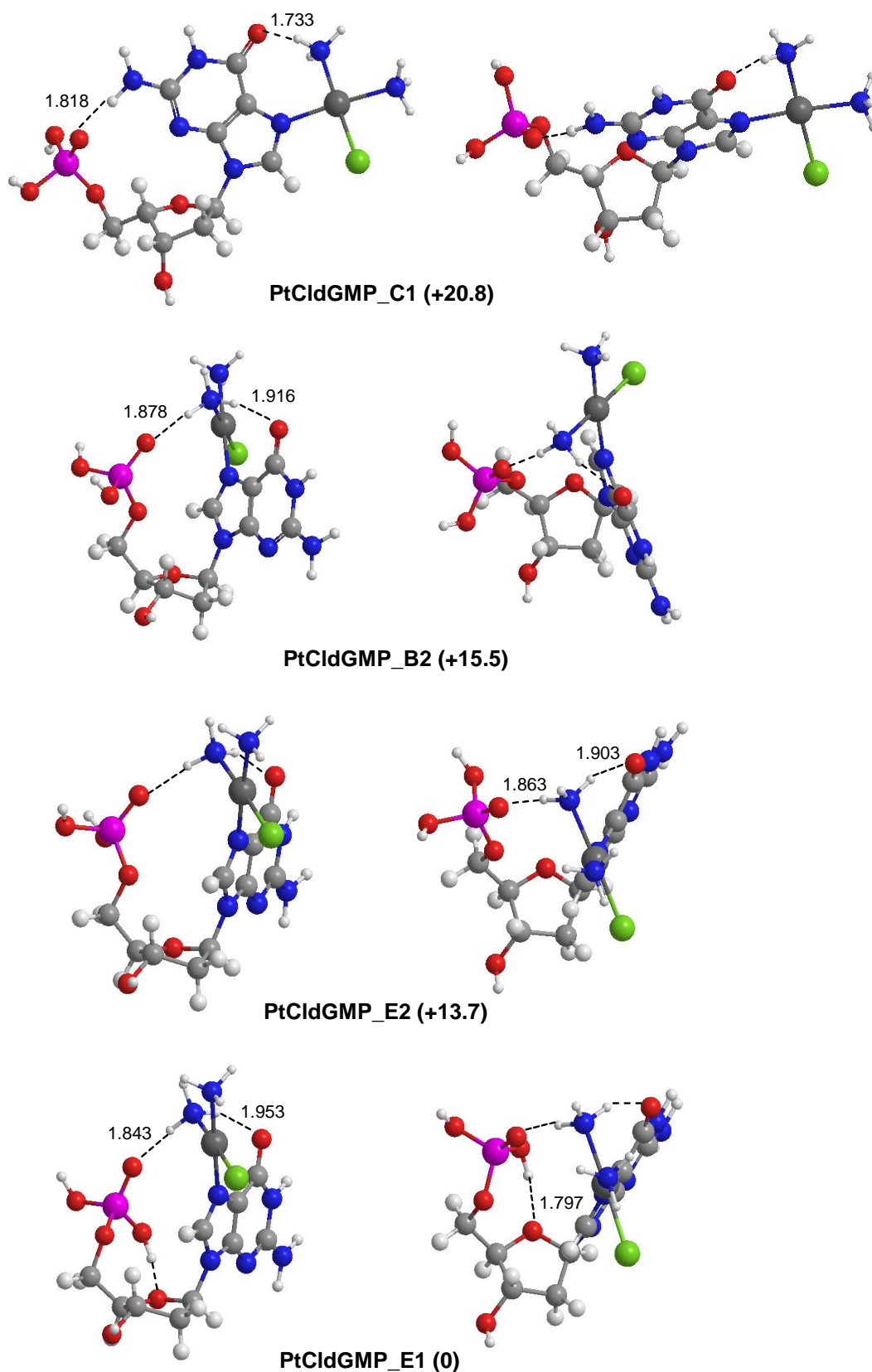


Figure 4. Geometries and relative free energies (kJ mol⁻¹) of representative *cis*-[PtCl(NH₃)₂(5'-dGMP)]⁺ structures calculated at the B3LYP/6-311G** level. Distances are in Å.

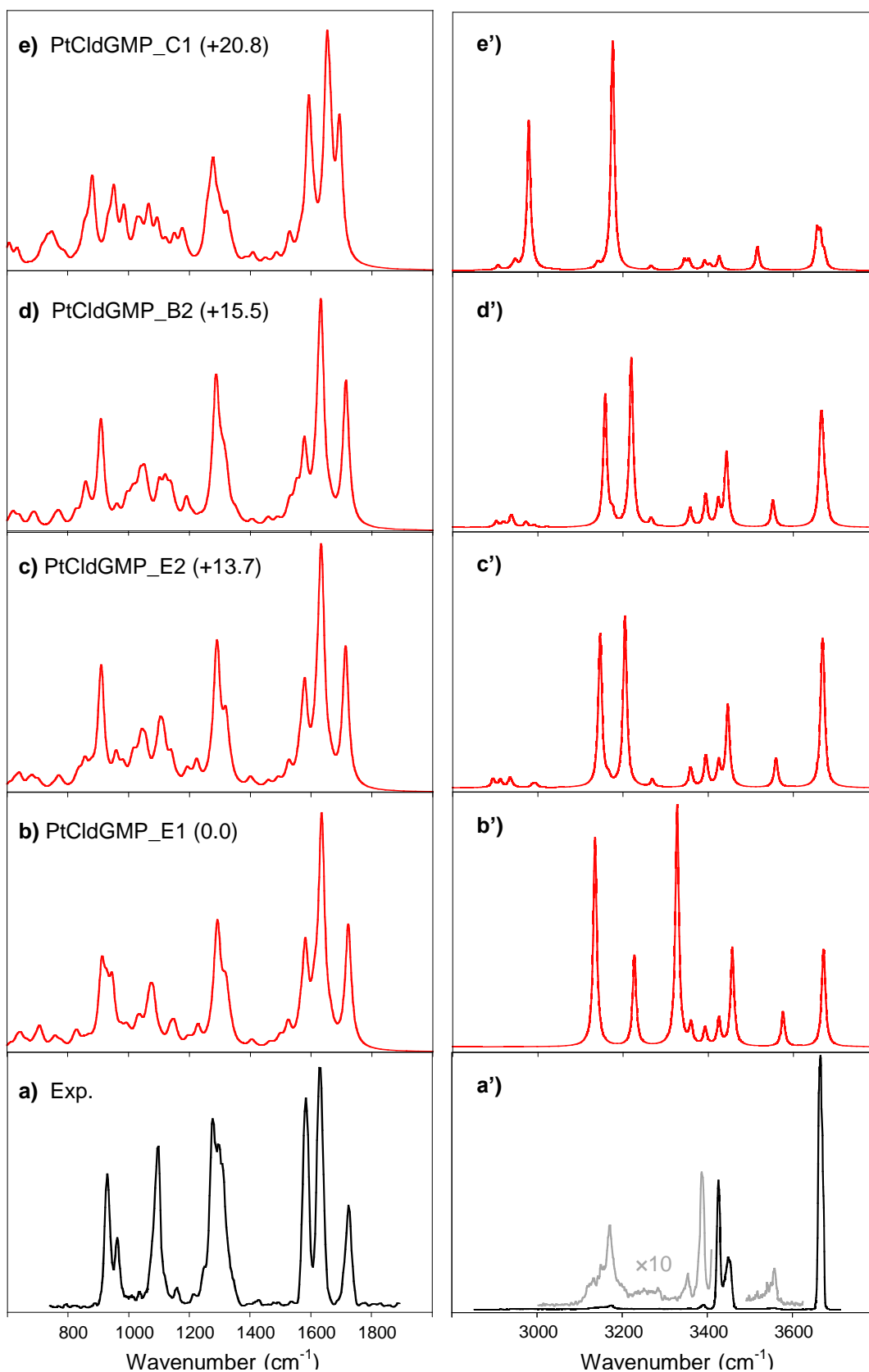


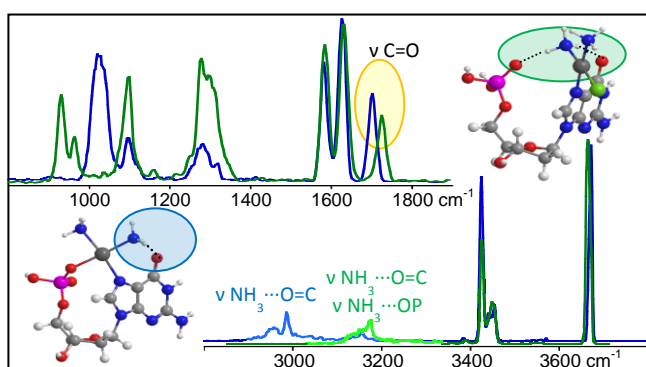
Figure 5. Experimental IRMPD spectrum of the cis -[PtCl(NH₃)₂(5'-dGMP)]⁺ complex (bottom) in both fingerprint (a) and X-H (X = C,N,O) stretch (a') region compared to IR

spectra of representative structures computed at the B3LYP/ 6-311G** level. See text for details.

Table of Contents Synopsis

The characterization of $cis\text{-[Pt(NH}_3\text{)}_2(5'\text{-dGMP-H})]^+$ ion points to macrochelate species resulting from the simultaneous interaction of the metal with both the N7 atom of the guanine residue and an O atom of the phosphate group. In contrast, IRMPD spectra of $cis\text{-[PtCl(NH}_3\text{)}_2(5'\text{-dGMP})]^+$ are consistent with a monodentate complex involving exclusively the N7 position of guanine. Also this species exhibits a compact shape due to the formation of two hydrogen bonds involving the same ammonia ligand.

Table of Contents Graphic



For Table of Contents Only

References

- (1) Rosenberg, B. *Cisplatin. Chemistry and Biochemistry of a Leading Anticancer Drug*; Verlag Helvetica Chimica Acta: Zürich, 1999.
- (2) Sherman, S. E.; Gibson, D.; Wang, A. H.; Lippard, S. J. *Science* **1985**, *230*, 412-417.
- (3) Sherman, S. E.; Lippard, S. J. *Chem. Rev.* **1987**, *87*, 1153-1181.
- (4) Sherman, S. E.; Gibson, D.; Wang, A. H. J.; Lippard, S. J. *J. Am. Chem. Soc.* **1988**, *110*, 7368-7381.
- (5) Bancroft, D. P.; Lepre, C. A.; Lippard, S. J. *J. Am. Chem. Soc.* **1990**, *112*, 6860-6871.
- (6) De Petris, A.; Ciavardini, A.; Coletti, C.; Re, N.; Chiavarino, B.; Crestoni, M. E.; Fornarini, S. *J. Phys. Chem. Lett.* **2013**, *4*, 3631-3635.
- (7) Chiavarino, B.; Crestoni, M. E.; Fornarini, S.; Scuderi, D.; Salpin, J. Y. *J. Am. Chem. Soc.* **2013**, *135*, 1445-1455.
- (8) Reily, M. D.; Marzilli, L. G. *J. Am. Chem. Soc.* **1986**, *108*, 8299-8300.
- (9) Reily, M. D.; Hambley, T. W.; Marzilli, L. G. *J. Am. Chem. Soc.* **1988**, *110*, 2999-3007.
- (10) Dijt, F. J.; Canters, G. W.; Den Hartog, J. H. J.; Marcelis, A. T. M.; Reedijk, J. *J. Am. Chem. Soc.* **1984**, *106*, 3644-3647.
- (11) Bernersprice, S. J.; Frenkiel, T. A.; Ranford, J. D.; Sadler, P. J. *J. Chem. Soc., Dalton Trans.* **1992**, 2137-2139.
- (12) MacAleese, L.; Maitre, P. *Mass Spectrom. Rev.* **2007**, *26*, 583-605.
- (13) Eyler, J. R. *Mass Spectrom. Rev.* **2009**, *28*, 448-467.
- (14) Fridgen, T. D. *Mass Spectrom. Rev.* **2009**, *28*, 586-607.
- (15) Polfer, N. C. *Chem. Soc. Rev.* **2011**, *40*, 2211-2221.
- (16) Lemaire, J.; Boissel, P.; Heninger, M.; Mauclaire, G.; Bellec, G.; Mestdagh, H.; Simon, A.; Le Caer, S.; Ortega, J. M.; Glotin, F.; Maitre, P. *Phys. Rev. Lett.* **2002**, *89*, 273002-273001.
- (17) Bakker, J. M.; Besson, T.; Lemaire, J.; Scuderi, D.; Maitre, P. *J. Phys. Chem. A* **2007**, *111*, 13415-13424.
- (18) Sinha, R. K.; Maitre, P.; Piccirillo, S.; Chiavarino, B.; Crestoni, M. E.; Fornarini, S. *Phys. Chem. Chem. Phys.* **2010**, *12*, 9794-9800.
- (19) Prell, J. S.; O'Brien, J. T.; Williams, E. R. *J. Am. Soc. Mass Spectrom.* **2010**, *21*, 800-809.
- (20) Lee, C.; Yang, W.; Parr, R. G. *Physical Reviews B* **1988**, *37*, 785-789.
- (21) Becke, A. D. *J. Chem. Phys.* **1993**, *98*, 5648-5652.

- (22) Frisch, M. J.; al., e.; Gaussian09, Revision C.01. See Supporting Information for complete citation. ed.
- (23) Hay, P. J.; Wadt, W. R. *J. Chem. Phys.* **1985**, *82*, 270-283.
- (24) Hay, P. J.; Wadt, W. R. *J. Chem. Phys.* **1985**, *82*, 299-310.
- (25) Wadt, W. R.; Hay, P. J. *J. Chem. Phys.* **1985**, *82*, 284-298.
- (26) Stevens, W. J.; Krauss, M.; Basch, H.; Jasien, P. G. *Can. J. Chem.* **1992**, *70*, 612-630.
- (27) Correia, C. F.; Balaj, P. O.; Scuderi, D.; Maitre, P.; Ohanessian, G. *J. Am. Chem. Soc.* **2008**, *130*, 3359-3370.
- (28) Scuderi, D.; Correia, C. F.; Balaj, O. P.; Ohanessian, G.; Lemaire, J.; Maitre, P. *ChemPhysChem* **2009**, *10*, 1630-1641.
- (29) Correia, C. F.; Clavaguera, C.; Erlekam, U.; Scuderi, D.; Ohanessian, G. *ChemPhysChem* **2008**, *9*, 2564-2573.
- (30) Chiavarino, B.; Crestoni, M. E.; Fornarini, S.; Lanucara, F.; Lemaire, J.; Maitre, P.; Scuderi, D. *Int. J. Mass Spectrom.* **2008**, *270*, 111-117.
- (31) Lanucara, F.; Crestoni, M. E.; Chiavarino, B.; Fornarini, S.; Hernandez, O.; Scuderi, D.; Maitre, P. *RSC Adv.* **2013**, *3*, 12711-12720.
- (32) Nei, Y. w.; Hallowita, N.; Steill, J. D.; Oomens, J.; Rodgers, M. T. *J. Phys. Chem. A* **2013**, *117*, 1319-1335.
- (33) Oomens, J.; Sartakov, B. G.; Meijer, G.; Von Helden, G. *Int. J. Mass Spectrom.* **2006**, *254*, 1-19.
- (34) Polfer, N. C.; Oomens, J. *Mass Spectrom. Rev.* **2009**, *28*, 468-494.
- (35) Brodbelt, J. S.; Wilson, J. J. *Mass Spectrom. Rev.* **2009**, *28*, 390-424.
- (36) Jones, W.; Boissel, P.; Chiavarino, B.; Crestoni, M. E.; Fornarini, S.; Lemaire, J.; Maitre, P. *Angew. Chem. Int. Ed.* **2003**, *42*, 2057-2059.
- (37) Chiavarino, B.; Crestoni, M. E.; Fornarini, S.; Lemaire, J.; Maitre, P.; MacAleese, L. *J. Am. Chem. Soc.* **2006**, *128*, 12553-12561.
- (38) Armentrout, P. B.; Rodgers, M. T.; Oomens, J.; Steill, J. D. *J. Phys. Chem. A* **2008**, *112*, 2248-2257.
- (39) Dopfer, O.; Lemaire, J.; Maitre, P.; Chiavarino, B.; Crestoni, M. E.; Fornarini, S. *Int. J. Mass Spectrom.* **2006**, *249*, 149-154.
- (40) Wu, R. H.; McMahon, T. B. *ChemPhysChem* **2008**, *9*, 2826-2835.
- (41) Chiavarino, B.; Crestoni, M. E.; Fornarini, S.; Lanucara, F.; Lemaire, J.; Maitre, P.; Scuderi, D. *Chem. Eur. J.* **2009**, *15*, 8185-8195.
- (42) Baer, T.; Dunbar, R. C. *J. Am. Soc. Mass Spectrom.* **2010**, *21*, 681-693.
- (43) Lanucara, F.; Chiavarino, B.; Crestoni, M. E.; Scuderi, D.; Sinha, R. K.; Maitre, P.; Fornarini, S. *Inorg. Chem.* **2011**, *50*, 4445-4452.
- (44) Salpin, J. Y.; Guillaumont, S.; Ortiz, D.; Tortajada, J.; Maitre, P. *Inorg. Chem.* **2011**, *50*, 7769-7778.

- (45) Lanucara, F.; Chiavarino, B.; Crestoni, M. E.; Scuderi, D.; Sinha, R. K.; Maitre, P.; Fornarini, S. *Int. J. Mass Spectrom.* **2012**, *330*, 160-167.
- (46) Crestoni, M. E.; Chiavarino, B.; Scuderi, D.; Di Marzio, A.; Fornarini, S. *J. Phys. Chem. B* **2012**, *116*, 8771-8779.
- (47) Lanucara, F.; Scuderi, D.; Chiavarino, B.; Fornarini, S.; Maitre, P.; Crestoni, M. E. *J. Phys. Chem. Lett.* **2013**, *4*, 2414-2417.
- (48) Dunbar, R. C.; Oomens, J.; Berden, G.; Lau, J. K. C.; Verkerk, U. H.; Hopkinson, A. C.; Siu, K. W. M. *J. Phys. Chem. A* **2013**, *117*, 5335-5343.
- (49) Lanucara, F.; Chiavarino, B.; Scuderi, D.; Maitre, P.; Fornarini, S.; Crestoni, M. E. *Chemical Communications* **2014**, *50*, 3845-3848.
- (50) Salpin, J.-Y.; MacAleese, L.; Chirot, F.; Dugourd, P. *Phys. Chem. Chem. Phys.* **2014**, *16*, 14127-14138.
- (51) Basch, H.; Krauss, M.; Stevens, W. J.; Cohen, D. *Inorg. Chem.* **1986**, *25*, 684-688.
- (52) Baik, M. H.; Friesner, R. A.; Lippard, S. J. *J. Am. Chem. Soc.* **2003**, *125*, 14082-14092.
- (53) Gidden, J.; Bowers, M. T. *J. Phys. Chem. B* **2003**, *107*, 12829-12837.
- (54) Chiavarino, B.; Crestoni, M. E.; Fornarini, S.; Scuderi, D.; Salpin, J.-Y. *J. Am. Chem. Soc.* **2013**, *135*, 10877-10877.
- (55) Wang, Y. S.; Chang, H. C.; Jiang, J. C.; Lin, S. H.; Lee, Y. T.; Chang, H. C. *J. Am. Chem. Soc.* **1998**, *120*, 8777-8788.
- (56) Kamariotis, A.; Boyarkin, O. V.; Mercier, S. R.; Beck, R. D.; Bush, M. F.; Williams, E. R.; Rizzo, T. R. *J. Am. Chem. Soc.* **2006**, *128*, 905-916.
- (57) Bakker, J. M.; Sinha, R. K.; Besson, T.; Brugnara, M.; Tosi, P.; Salpin, J. Y.; Maitre, P. *J. Phys. Chem. A* **2008**, *112*, 12393-12400.
- (58) Bakker, J. M.; Salpin, J. Y.; Maitre, P. *Int. J. Mass Spectrom.* **2009**, *283*, 214-221.
- (59) Scuderi, D.; Le Barbu-Debus, K.; Zehnacker, A. *Phys. Chem. Chem. Phys.* **2011**, *13*, 17916-17929.